Modeling of Leakage Currents in Ultra Shallow Junctions

Andreas Schenk, Artur Scheinemann

ETH Zürich, Integrated Systems Laboratory

Outline

- Introduction
- Leakage mechanisms and physical models for TCAD
- Extended defects: DLTS data and reverse currents
- DLTS device simulation
- Model for generation via dislocation loops
- Conclusion

Introduction

USJ formation in complex CMOS processes:

- Cocktail implants with a variety of elements
- Reduced thermal budgets ⟶ bigger amounts of crystal damage

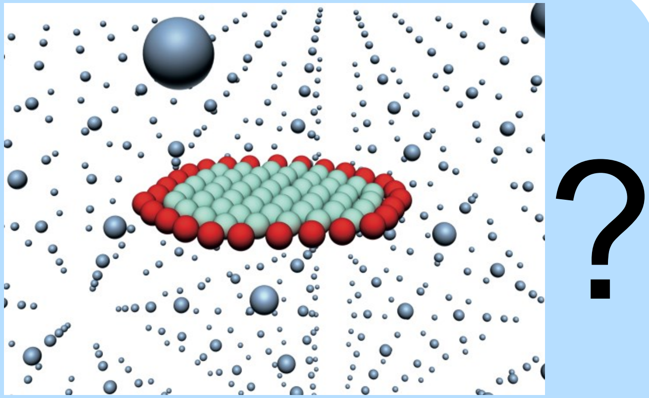

Electrical activity of EDs and their interaction with impurities

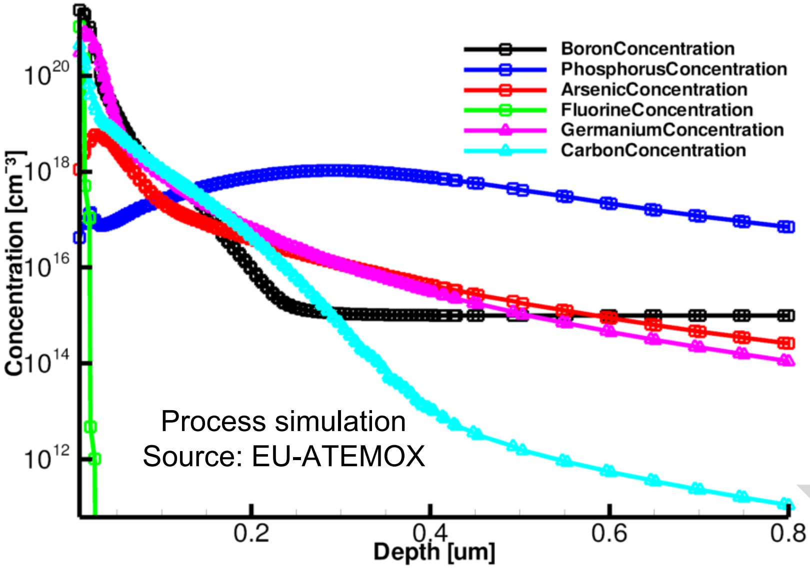

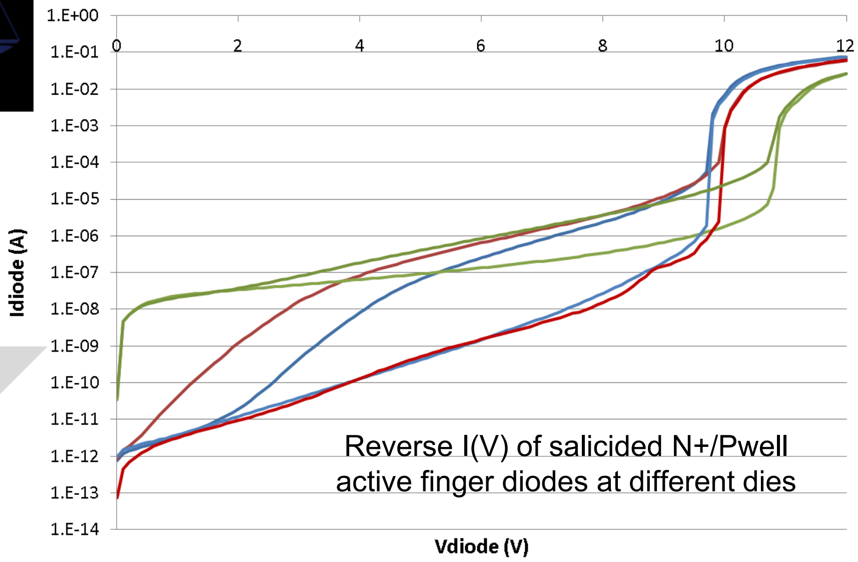

IV-characteristics hard to interprete and predict

Leakage mechanisms and physical models for TCAD

Rates of important leakage mechanisms in drain junction

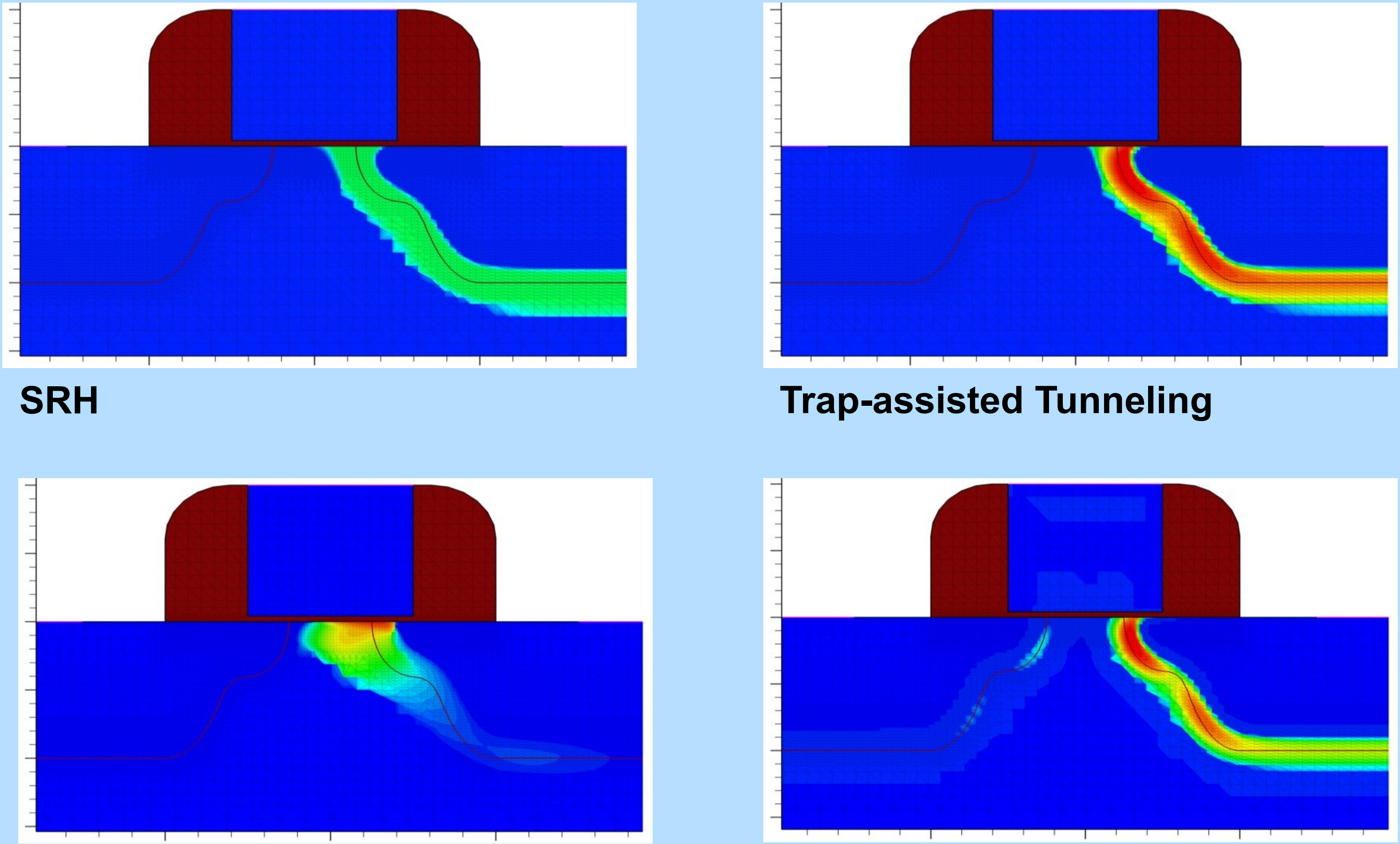

SRH

Trap-assisted Tunneling

Impact Ionization

Band-to-band Tunneling

Trap-assisted tunneling

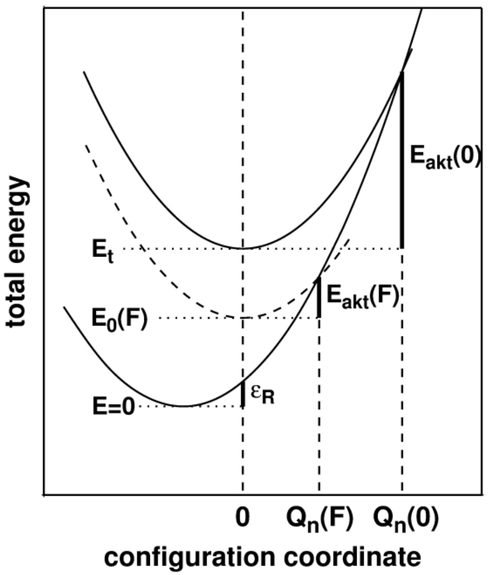

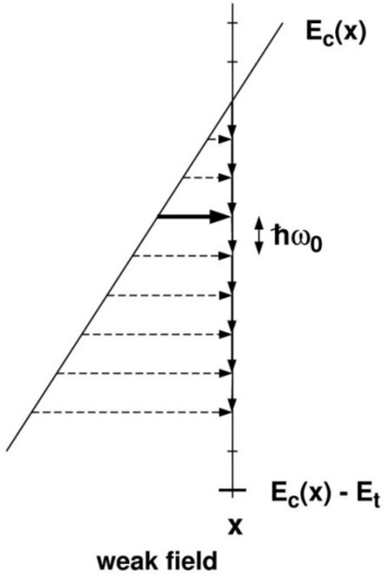

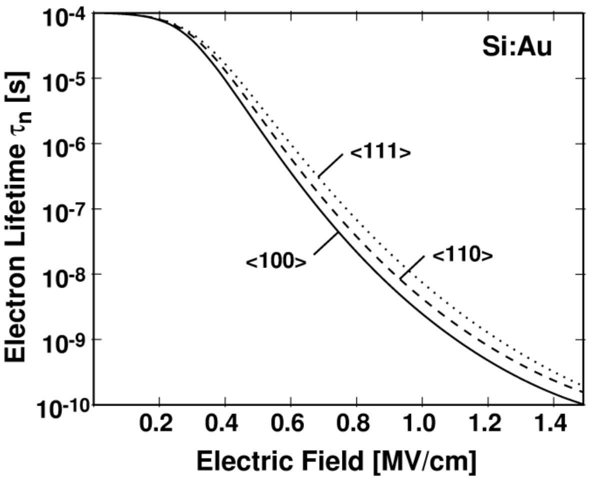

- … is a field-enhanced multi-phonon generation process. →Field-enhancement factors for inverse lifetimes.
- Analytical model for single-level centers, eff. phonon mode, LT approximation

$$\tau_n^{-1}(\vec{x}) = \tau_n^{-1}(\vec{x}, F=0)\, g_n(F(\vec{x}))$$

$$g_n(F(\vec{x})) = \left(1 + \frac{(\hbar\omega_0)^{\frac{3}{2}}\sqrt{E_t - E_0}}{E_0\hbar\omega_0}\right)^{-\frac{1}{2}} \frac{(\hbar\omega_0)^{\frac{3}{4}}(E_t - E_0)^{\frac{1}{4}}}{2\sqrt{E_t E_0}} \left(\frac{\hbar\omega_0}{kT}\right)^{\frac{3}{2}} \times e^{-\frac{E_t - E_0}{\hbar\omega_0} + \frac{\hbar\omega_0 - kT}{2\hbar\omega_0} + \frac{2E_t + kT}{2\hbar\omega_0}\ln\frac{E_t}{\varepsilon_R} + \frac{E_t - E_0}{kT} - \frac{4}{3}\left(\frac{E_t - E_0}{\hbar\omega_0}\right)^{\frac{3}{2}}}$$

A. Schenk, "A Model for the Field and Temperature Dependence of Shockley-Read-Hall Lifetimes in Silicon", Solid-State Electronics, vol. 35 (11), 1585-96, (1992).

Coupled defect-level generation

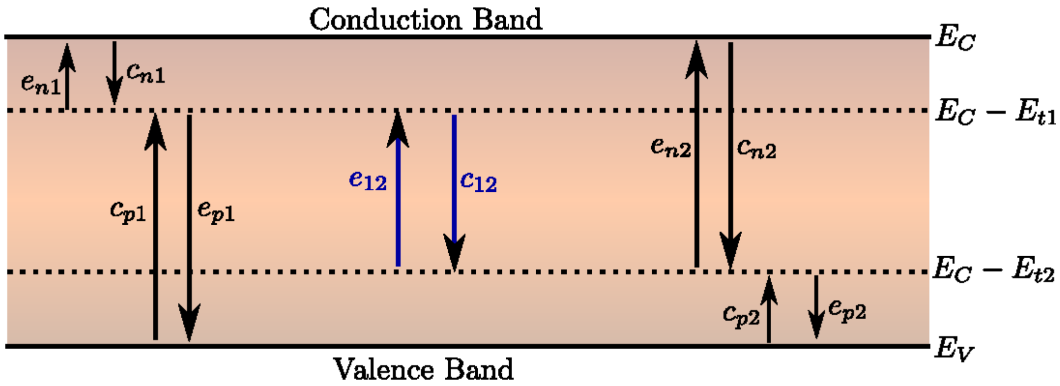

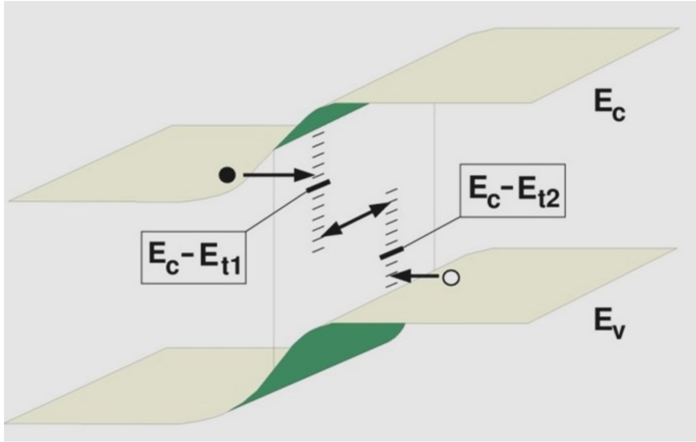

$$R = R_1 + R_2 + \left(\sqrt{R_{12}^2 - S_{12}} - R_{12}\right) \times$$

$$\times \frac{\tau_{n1}\tau_{p2}(n+n_2)(p+p_1) - \tau_{n2}\tau_{p1}(n+n_1)(p+p_2)}{r_1 r_2}$$

- Modified SRH statistics. Analytical model for 2 levels possible.
- Multi levels and coupling are basic ideas for GR model for extended defects.

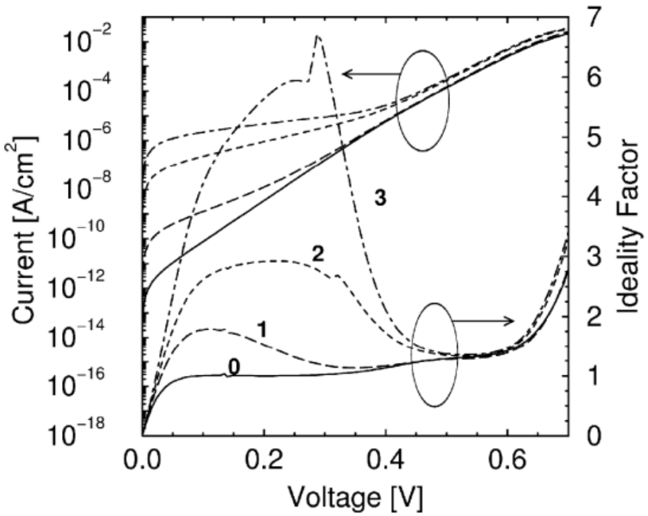

A. Schenk and U. Krumbein, "Coupled defect-level recombination: Theory and application to anomalous diode characteristics", J. Appl. Phys. vol. 78 (5), pp. 3185 - 3192 (1995).

O. Breitenstein, P. Altermatt, K. Ramspeck, M. A. Green, Jianhua Zhao, and A. Schenk, "Interpretation of the commonly Observed I-V characteristics of c-Si cells having ideality factor larger than two", 4th World Conference on Photovoltaic Energy Conversion (WCPEC 2006), Hilton Waikoloa, Hawai, May 7-12, 2006, pp. 625 - 628.

Benchmark

- Simulation benchmark for planar bulk 30nm nMOSFET with 1nm EOT.
- Defects increase SRH and TAT on top of DIBL. Onset of BTBT due to high halo doping (for suppression of DIBL).

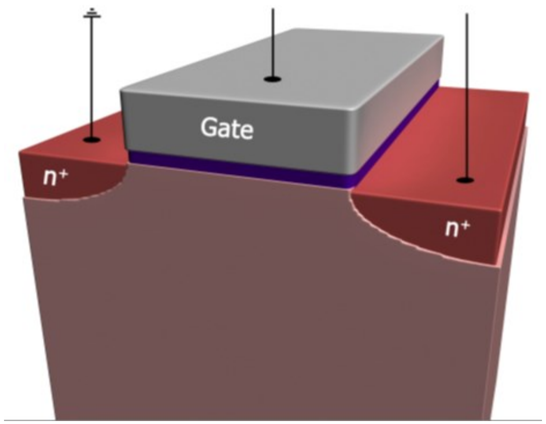

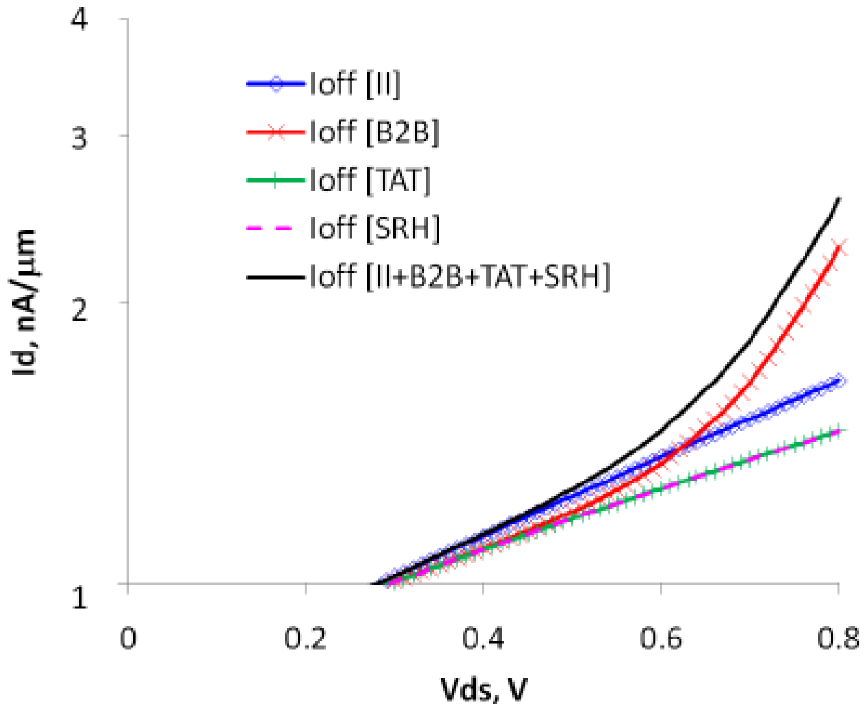

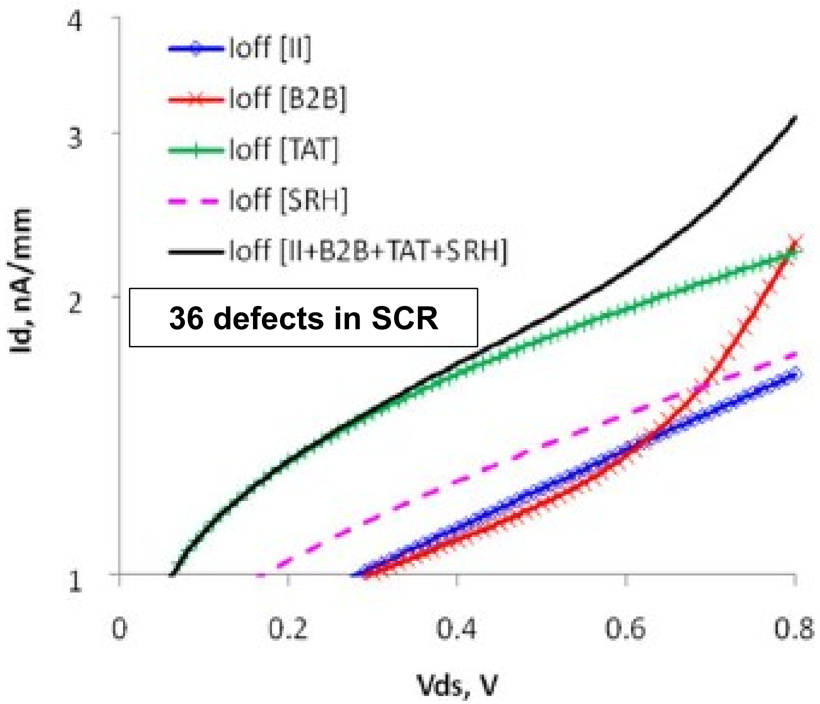

V. Moroz and M. Choi, "Impact of stress and defects on advanced junction leakage", ECS Trans. 33(11), 221-236 (2010).

Extended defects: DLTS data and reverse currents

Zoo of Extended Defects

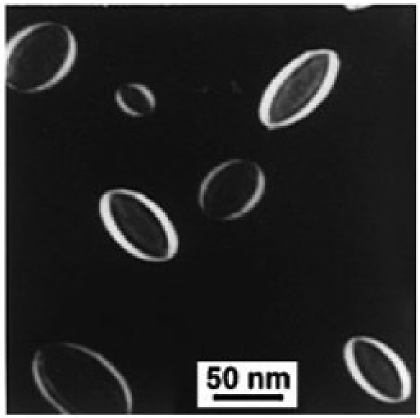

Dislocation Loops

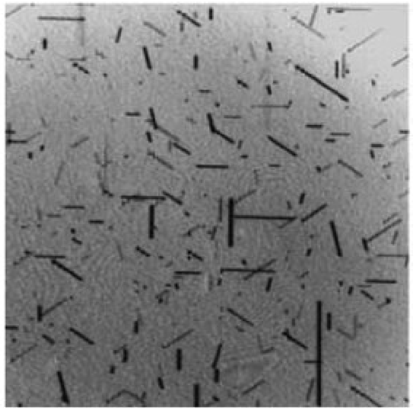

{311} defects

- Complex variety of extended defects with dependence on
  - Implant conditions
  - Thermal budget
  - Mechanical stress
- Interactions with point-like defects contained in the crystal

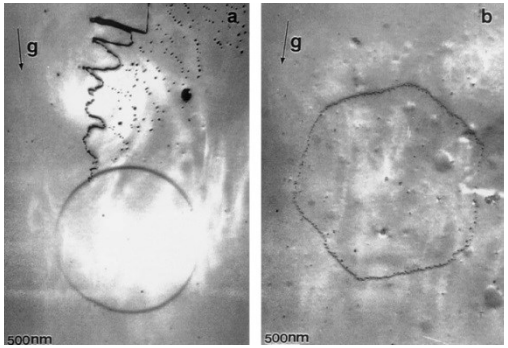

Copper precipitates on dislocations

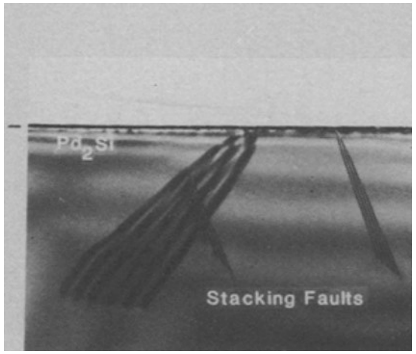

Stacking faults

Source:
Claverie et. Al., Materials Science in Semiconductor Processing 3, (2000)
Calvo et. Al., NIM B (2004)
K. Sumino, Materials Science & Engineering B (2000)

ED energy levels

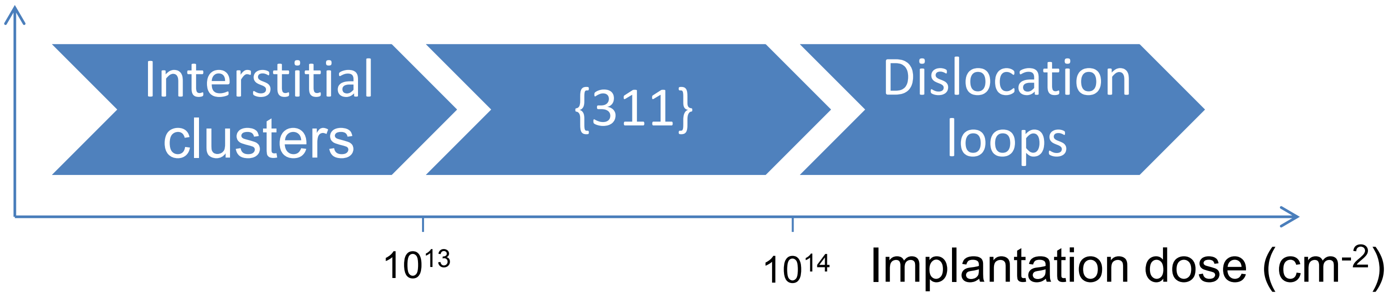

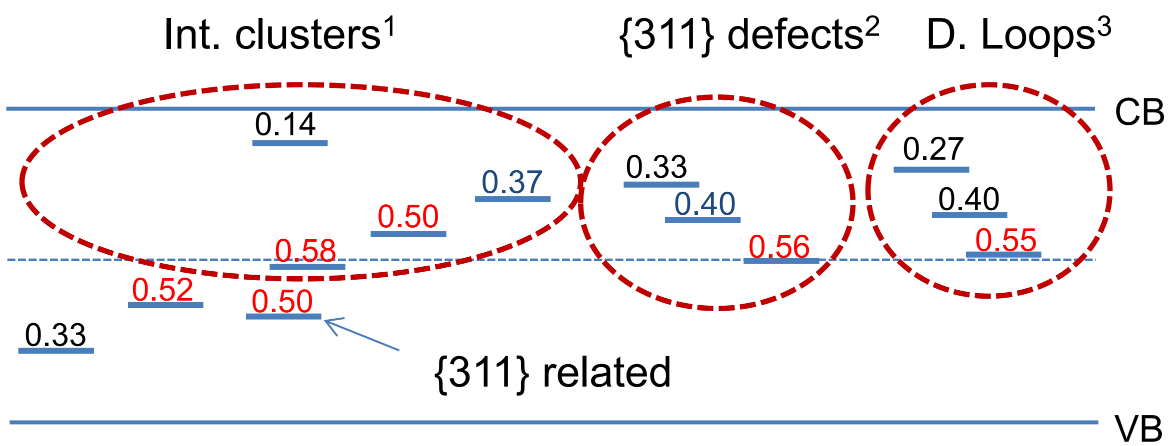

- Several studies have assigned a number of deep levels to extended defects.
- Some apparently similar electrical defects might be associated to different structural defects.

Source: Fuccio Cristiano et al. (LAAS), EU-ATEMOX

[1]Benton *et al.* JAP 84 (1998) 4749, and Schmidt *et al.* JAP 88 (2000) 2309
[2]Libertino *et al*. PRB 63 (2001) 195206 Schmidt *et al.* JAP 88 (2000) 2309
[3]Ayres *et al*. APL 71 (1990) 2214, JAP 71 (1992) 2702, and Evans-Freeman *et al*, JAP (2003)

Dislocation Loops: findings from literature

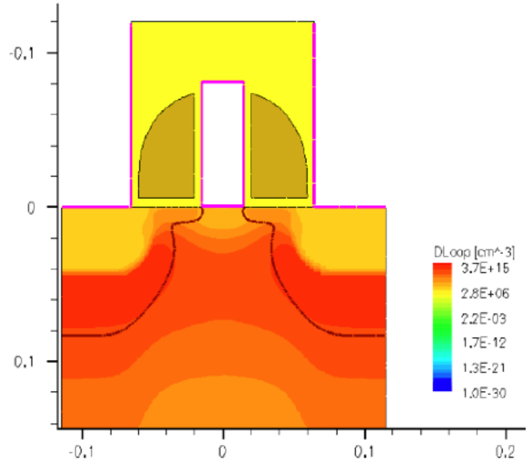

- Simulation of # interstitials in DLs that survive millisecond anneal.
- Low defect density within 40 nm from surface (amorphized and recrystallized).
- DLs must be in SCR for effect on leakage current.

V. Moroz and M. Choi, "Impact of stress and defects on advanced junction leakage", ECS Trans. 33(11), 221-236 (2010).

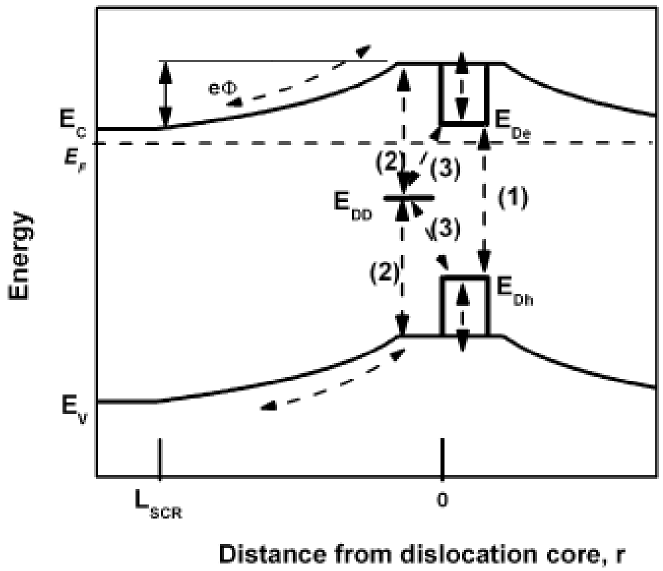

Diagram of the recombination processes at a **dislocation defect in silicon**. Levels E_{De} and E_{Dh} are shallow levels due to the intrinsic dislocation core itself. E_{DD} is an impurity introduced deep level. Important to notice is the Coulomb barrier Φ induced through the majority carrier line charges captured at the dislocation. L_{scr} indicates the radius of the space charge region around the dislocation. Picture extracted from **M. Seibt et al.**, Appl. Phys. A, 96: 235–253, 2009.

Dislocation Loops: recent DLTS data

3 x 10^{14} Ge cm^{-2}/1000°C

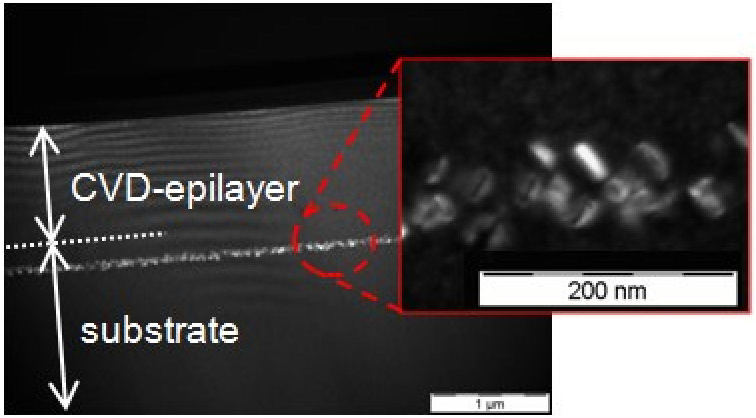

Source: Fuccio Cristiano et al. (LAAS), EU-ATEMOX, 2012

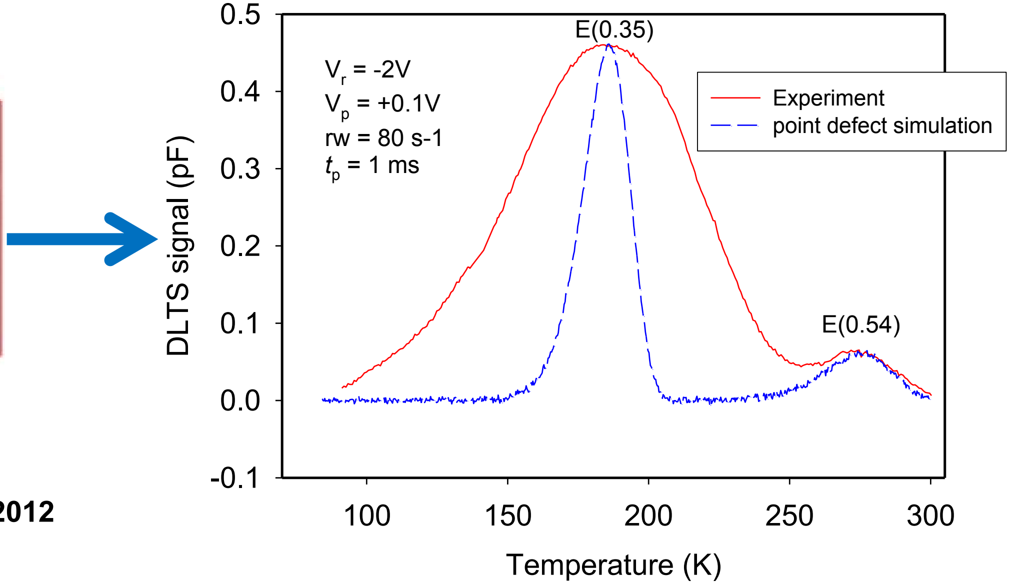

- Evidence of DLs from TEM of Schottky diodes with CVD-epilayer
- Broad spectra, [E(0.35 ± 0.15) eV; $\sigma = 2 \times 10^{-15}$ cm^2], $N_T = 1.7 \times 10^{13}$ cm^{-3}
- Weak E(0.54) peak compared to samples with {311} and ICs, where it is the strongest

Dislocation Loops: reverse currents

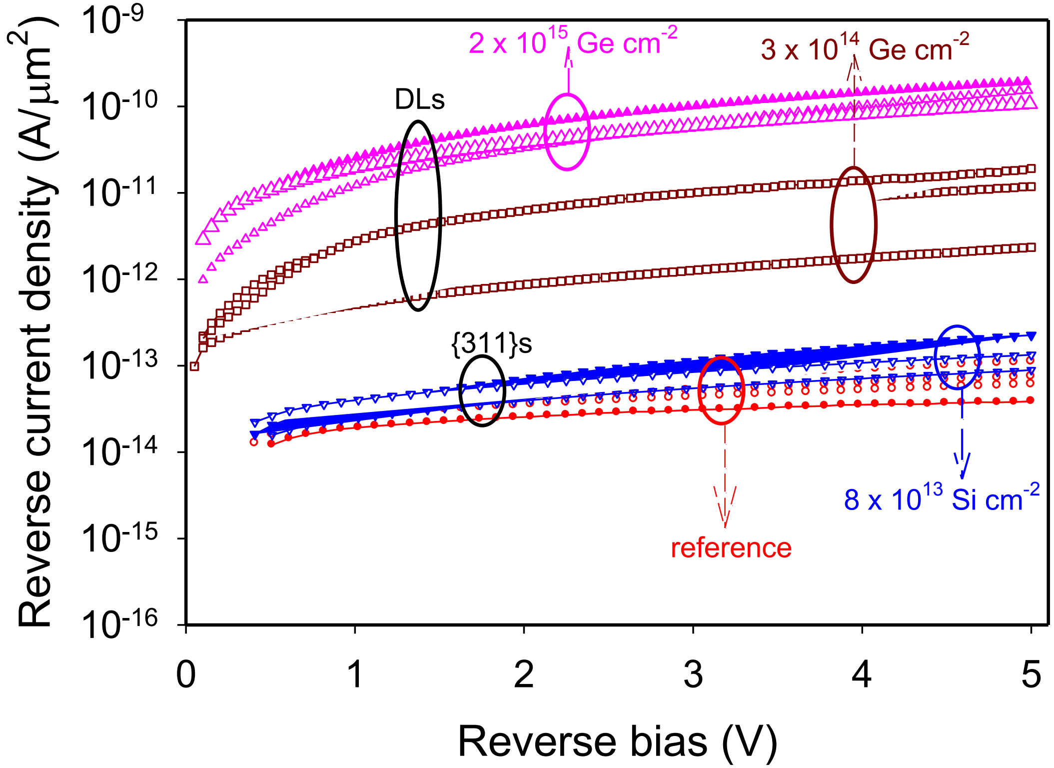

Source: Fuccio Cristiano et al. (LAAS), EU-ATEMOX, 2012

- Only small increase of leakage current in samples with {311} defects → contribution of level E(0.54) is not significant
- Strong increase in leakage current for the samples with DLs → E(0.35± 0.15) eV dominant → DLs much more efficient GR centers

DLTS device simulation

Transient Spectroscopy (principle)

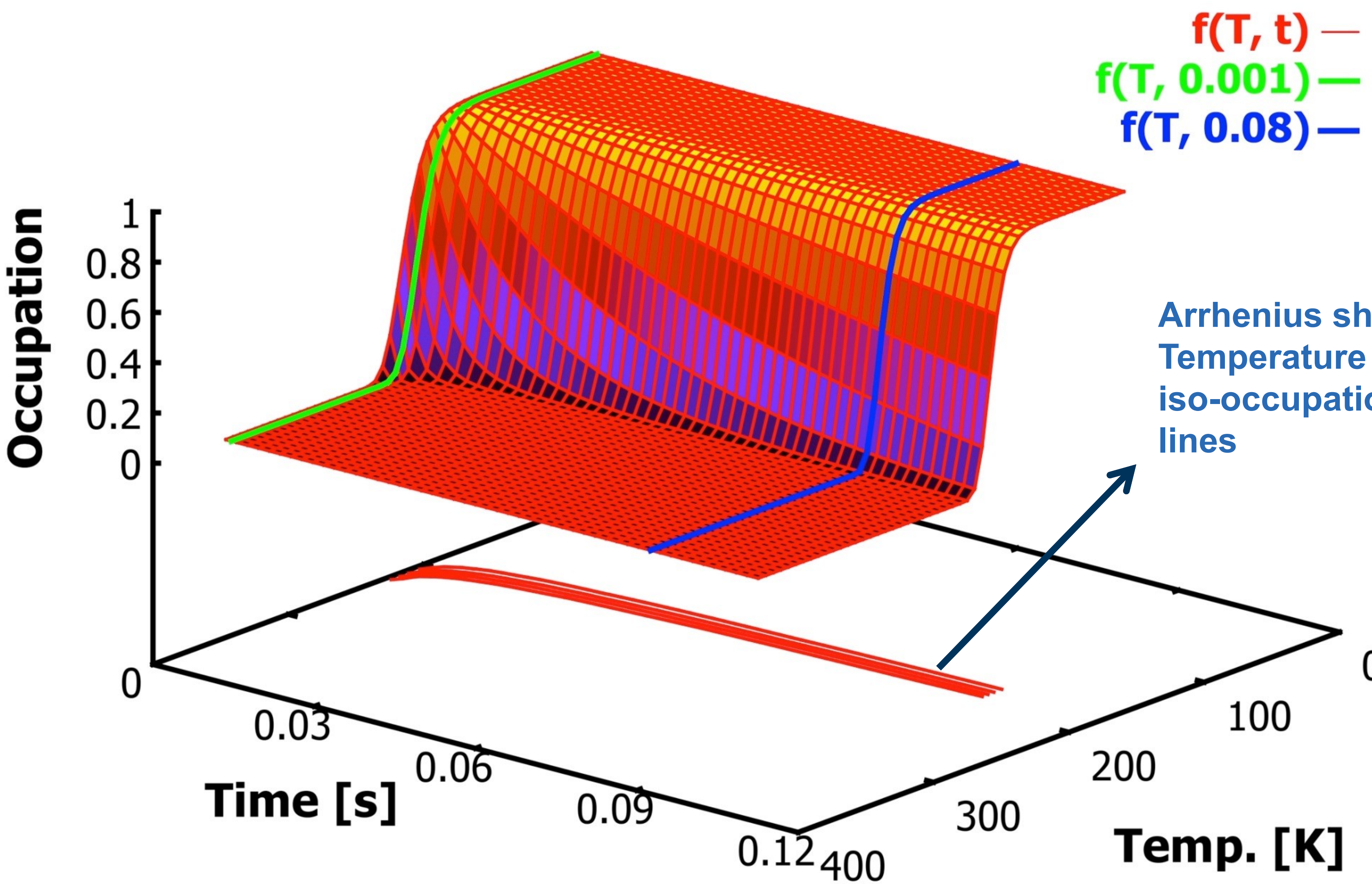

Arrhenius shift in Temperature of iso-occupational lines

Defect Occupation

- Transition between occupied / unoccupied state is governed by microscopic properties of the defect: E_T , $\sigma_{n,p}$

$$\frac{\mathrm{d}n(t,\mathrm{T})}{\mathrm{d}t} = -n(t,\mathrm{T})\left[e_n(\mathrm{T}) + c_p(\mathrm{T})\right] + \left(N_T - n(t,\mathrm{T})\right)\left[e_p(\mathrm{T}) + c_n(\mathrm{T})\right]$$

Analytical solution by omission of:
e_p, c_n, c_p

$$n(t,\mathrm{T}) = n(t_0,\mathrm{T})e^{-t\cdot e_n(\mathrm{T})}$$

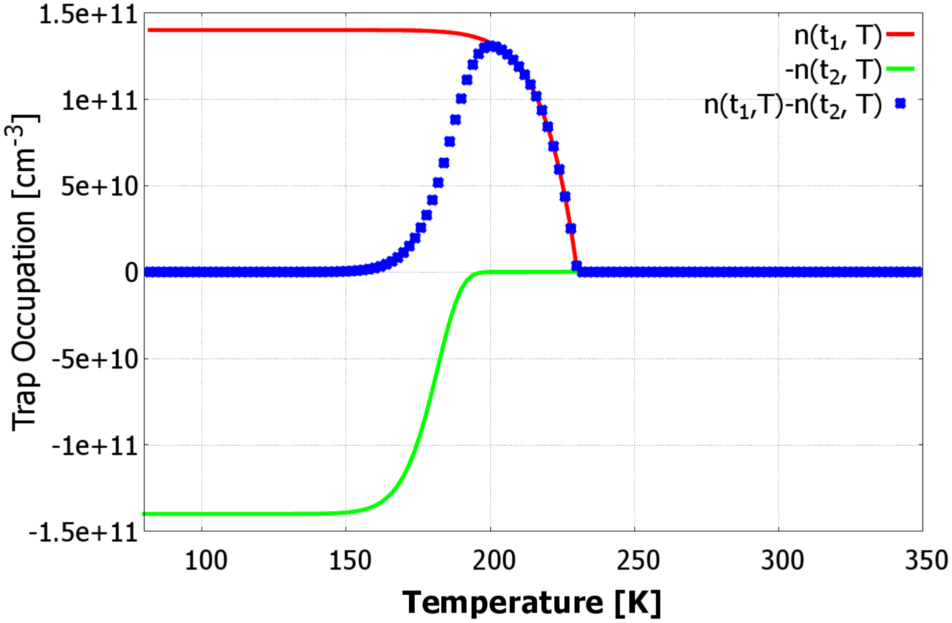

Defect Occupation (2)

Analytical solution is only valid under simplifying assumptions:

- $e_n \gg e_p, c_n, c_p$ or at least $e_v \gg c_v$, otherwise free carrier profiles needed.
- For different coupled defect species no analytical solution is possible.
- Spatial distribution of defect profiles $N_T(\mathbf{r})$ can not be evaluated.

Numerical integration of $n(t,T)$ from initial condition

$$n(t_i, \mathrm{T}) = n(t_{i-1}, \mathrm{T}) + \Delta t \cdot \frac{\mathrm{d}n}{\mathrm{d}t}$$

Simple numerical integration of n(t,T) leaving N_T constant and omitting carrier capture →

Using carrier and defect profiles obtained by process and device simulation to run integration on 1D/2D device

← Use of advanced device simulation software for transient simulations of DLTS profiles

Defect Occupation (3)

Sentaurus-Device DLTS simulation of Schottky diode with CVD-epilayer:

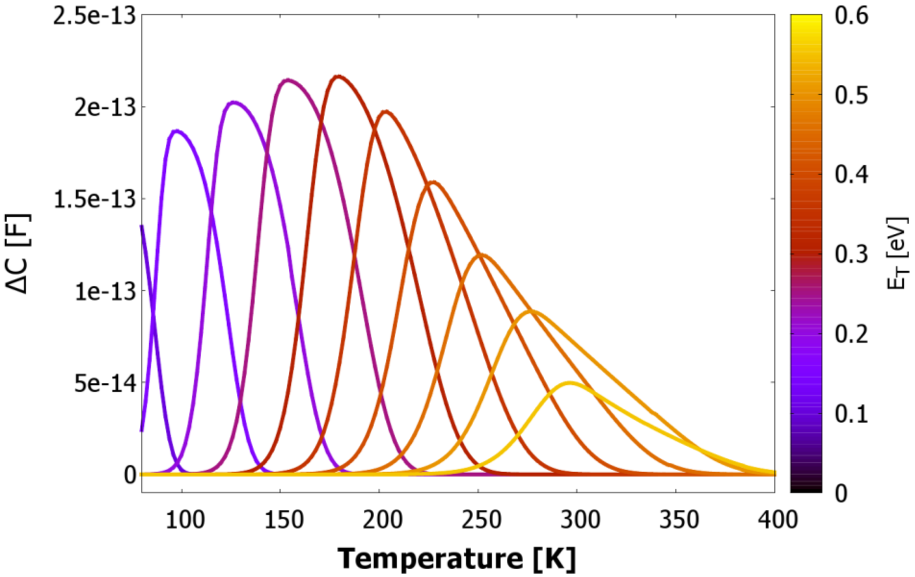

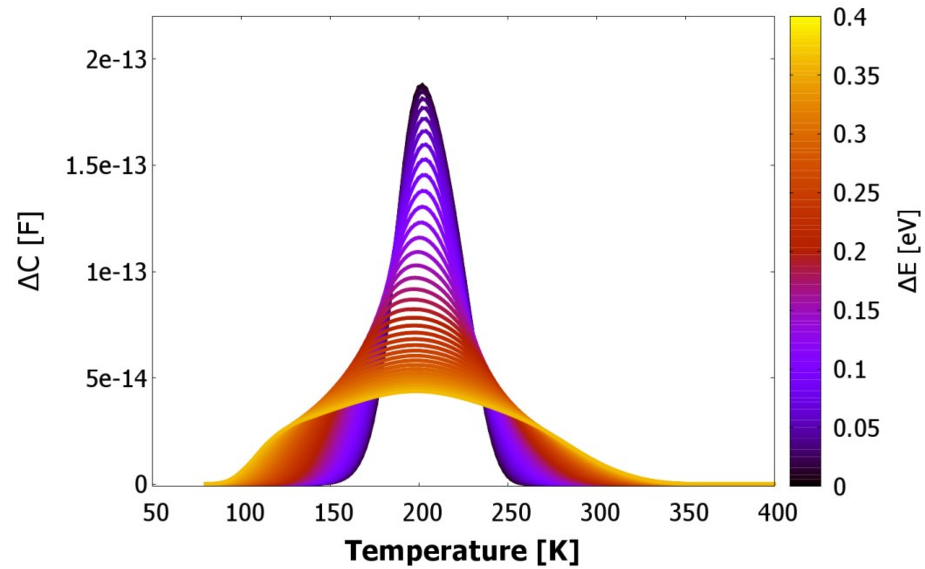

- Shift of the level E_T from mid-gap to E_C shifts the DLTS peak to lower temperatures. Reason: T_{max} "~" E_C - E_T
- Peak height reaches a maximum where $E_T \approx E_F$. Reason: also hole and capture processes in transient device simulation.

- 10 uncoupled levels around $E_T = E_C$ – 0.35 eV, $N_{T,i}$ = 1e12 cm^{-3}, σ_n = 1e-15 cm^2.
- Distributed over energy interval *ΔE*.
- With increasing *ΔE* the DLTS peak broadens and slightly shifts to lower T.

Coupling of 2 defect levels

- Numerical integration is easily extended to 2 defect levels with mutual coupling.
- $E_{T1} = E_C - 0.35$ eV, $E_{T2} = E_C - 0.55$ eV, $N_1 = 1e12$ cm^{-3}, $N_2 = 1.5e12$ cm^{-3} , $\sigma_n = 1e\text{-}15$ cm^2
- With increasing coupling strength one DLTS peak is “absorbed” by the peak closest to the band. → Peak of the mid-gap level disappears.

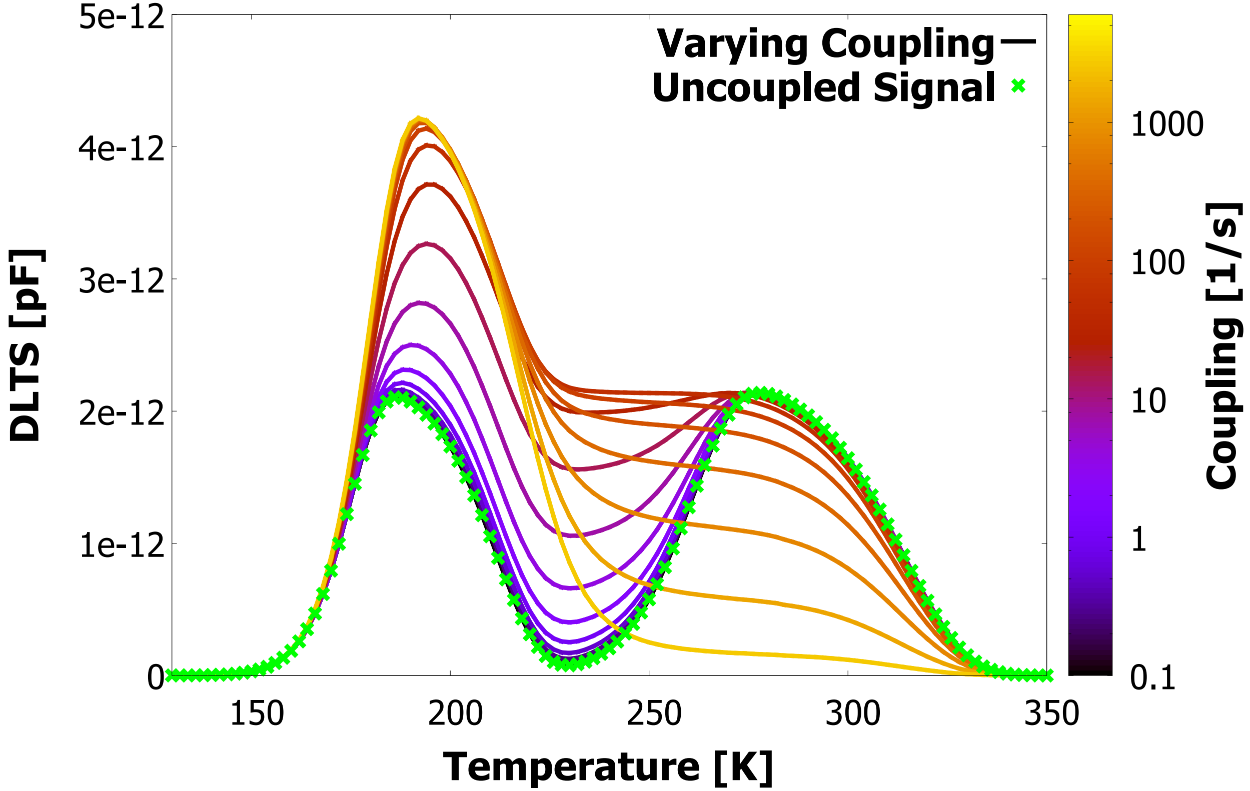

Coupling of L defect levels

$$
\begin{aligned}
\frac{\mathrm{d}n_1}{\mathrm{d}t} &= -(e_{n,1}+c_{p,1})n_1(t)+(e_{p,1}+c_{n,1})(N_1-n_1(t)) \\
&\quad +\tilde{c}_1(N_1-n_1(t))n_2(t)-\tilde{e}_1(N_2-n_2(t))n_1(t) \\
&\vdots \\
\frac{\mathrm{d}n_i}{\mathrm{d}t} &= -(e_{n,i}+c_{p,i})n_i(t)+(e_{p,i}+c_{n,i})(N_i-n_i(t)) \\
&\quad -\tilde{c}_{i-1}(N_{i-1}-n_{i-1}(t))n_i(t)+\tilde{e}_{i-1}(N_i-n_i(t))n_{i-1}(t) \\
&\quad +\tilde{c}_i(N_i-n_i(t))n_{i+1}(t)-\tilde{e}_i(N_{i+1}-n_{i+1}(t))n_i(t) \\
&\vdots \\
\frac{\mathrm{d}n_L}{\mathrm{d}t} &= -(e_{n,L}+c_{p,L})n_L(t)+(e_{p,L}+c_{n,L})(N_L-n_L(t)) \\
&\quad -\tilde{c}_{L-1}(N_{L-1}-n_{L-1}(t))n_L(t)+\tilde{e}_{L-1}(N_L-n_L(t))n_{L-1}(t)
\end{aligned}
$$

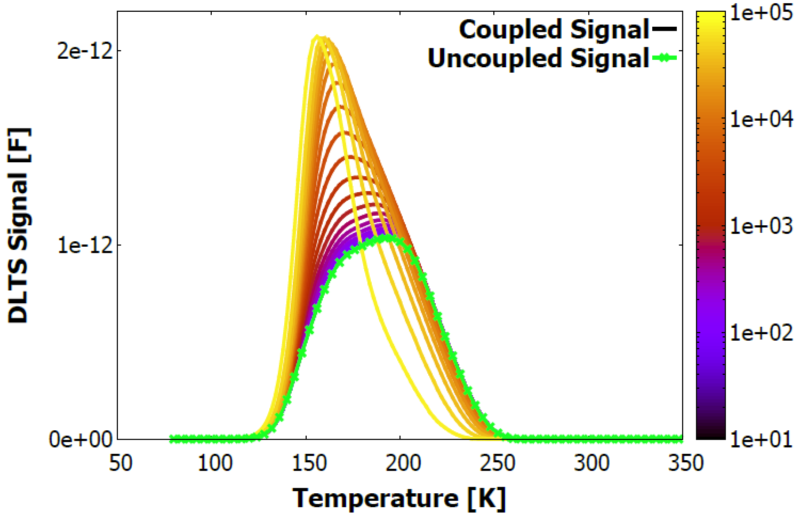

- 10 coupled levels around $E_T = E_C - 0.35$ eV, $N_{T,i}$ = 1e12 cm^{-3}, σ_n = 1e-15 cm^2.
- With increasing coupling rate the peak height grows up to x2 and the maximum shifts to the position of the peak closest to the band.

Model for generation via dislocation loops

DLTS peak analysis with S-Device (Schottky diode)

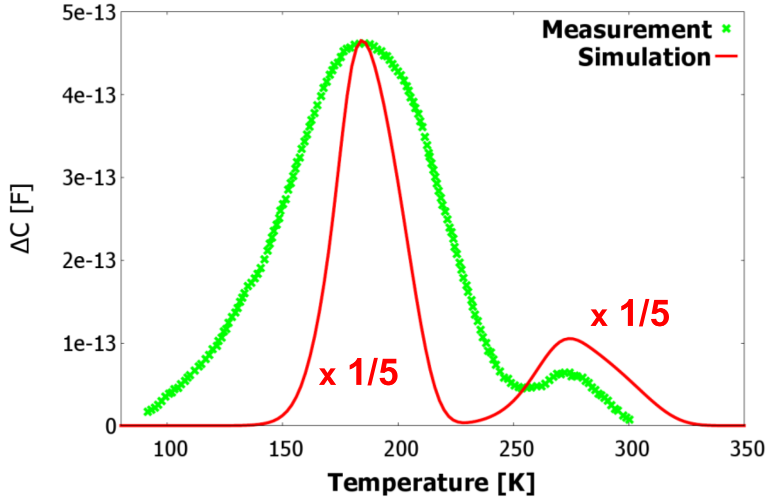

- 2 levels at $E_T = E_C - 0.35$ eV and mid-gap, $\sigma_n = 1\text{e-}15\ \text{cm}^2$, concentration taken from process simulation assuming one point defect on each peripheral site of the DLs.
- Concentration then scaled by 1/5.

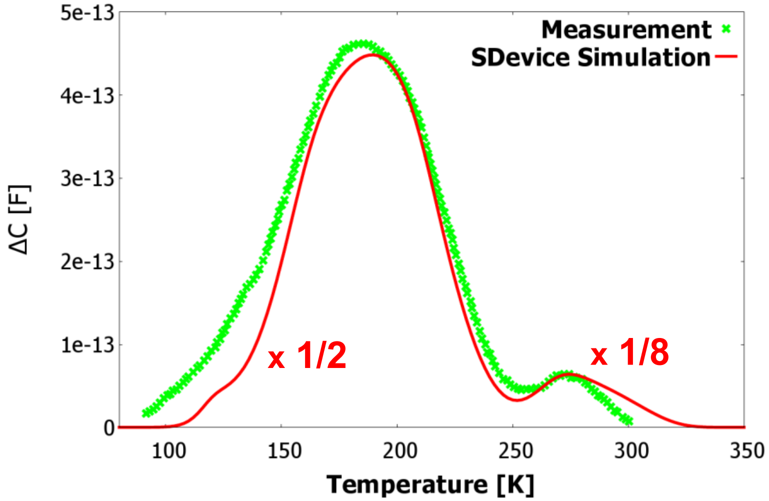

- Best fit of main peak assuming 30 uncoupled levels around $E_T = E_C - 0.33$ eV, $\sigma_n = 1\text{e-}15\ \text{cm}^2$.
- Levels distributed over energy interval $\Delta E = 0.2$ eV .
- Peak tails are not well reproduced.
- Peak could be related to the famous "C-line" observed at line dislocations, but broadening much larger here (200meV instead of 10-50meV)

Experimental data: Fuccio Cristiano et al. (LAAS), EU-ATEMOX, 2012

Leakage current

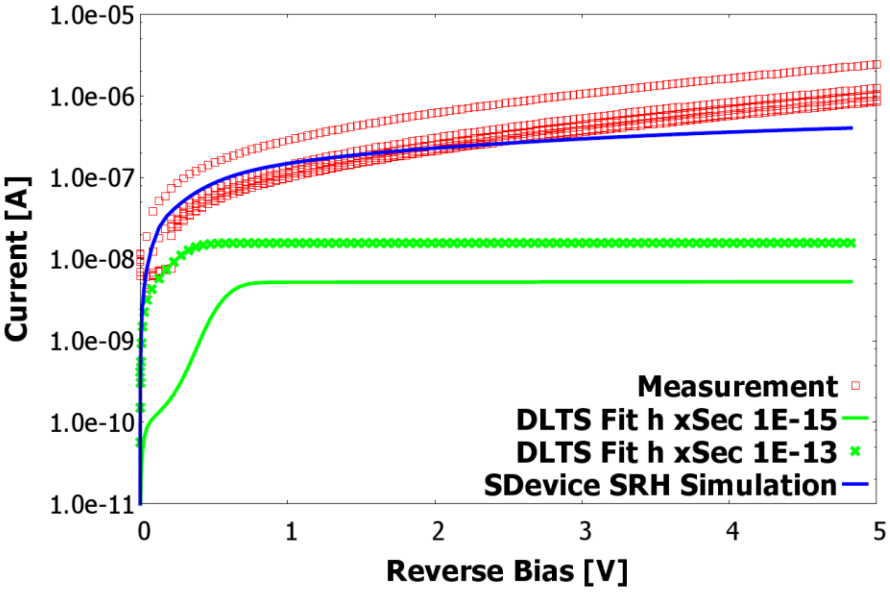

- Use "best fit": $E_T = E_C - 0.33$ eV, σ_n = 1e-15 cm^2, ΔE = 0.2 eV, scaled concentrations and two values for σ_p.
- Simulated current by far smaller than measured!
- Slope constant above 0.5V since DL profile fully contained in the SCR (according to process simulation).
- Ordinary SRH rate with micro-second lifetimes reproduces the measured current, but not the slope (wrong electrostatics, TAT?).
- **Suspicion**: current is not due to DLs, but originates from homogeneous background point-defect concentration.

Model refinement

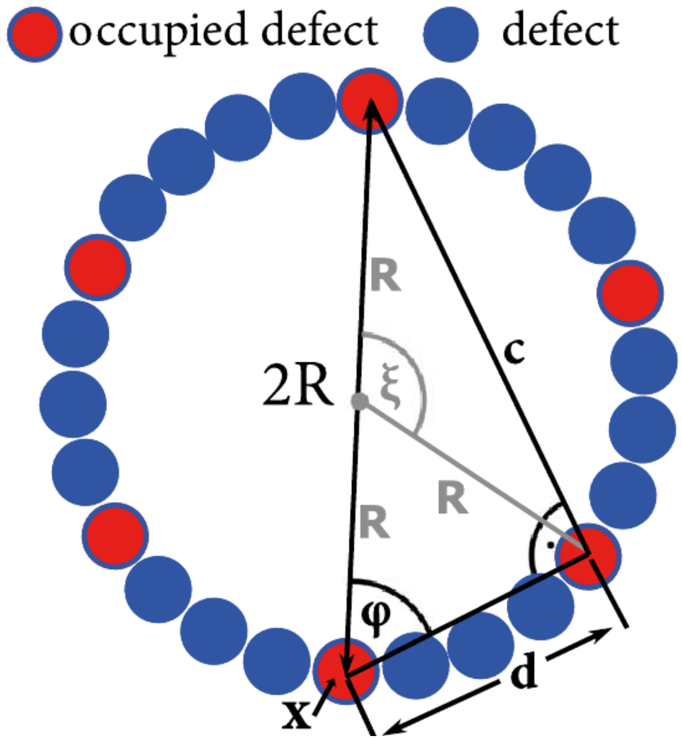

- Main question: What causes the broadening of the DLTS peak in emission? What is the origin of a *ΔE* (ladder of levels or constant DOS, resp.)?
- Deep impurity band not likely (need a multi-phonon process, i.e. strong e-ph-coupling, localized states).
- Shallow 1D bands only change E_T.
- Assume full (only for simplicity) decoration by point-like deep centers along the perimeter of a circular (for simplicity) DL.
- Coulomb repulsion energy for isotropic occupation with electrons:

$$E^{\text{even}}_{\text{Coulomb}} = \frac{e^2}{4\pi\epsilon_0\epsilon}\frac{1}{2R}\left\{1 + \sum_{i=1}^{\frac{n_D-2}{2}} \frac{2}{\cos\left(\frac{i\pi}{n_D}\right)}\right\}$$

$$E^{\text{odd}}_{\text{Coulomb}} = \frac{e^2}{4\pi\epsilon_0\epsilon}\frac{1}{2R}\sum_{i=1}^{\frac{n_D-1}{2}} \frac{2}{\sin\left(\frac{i\pi}{n_D}\right)}$$

Model refinement (2)

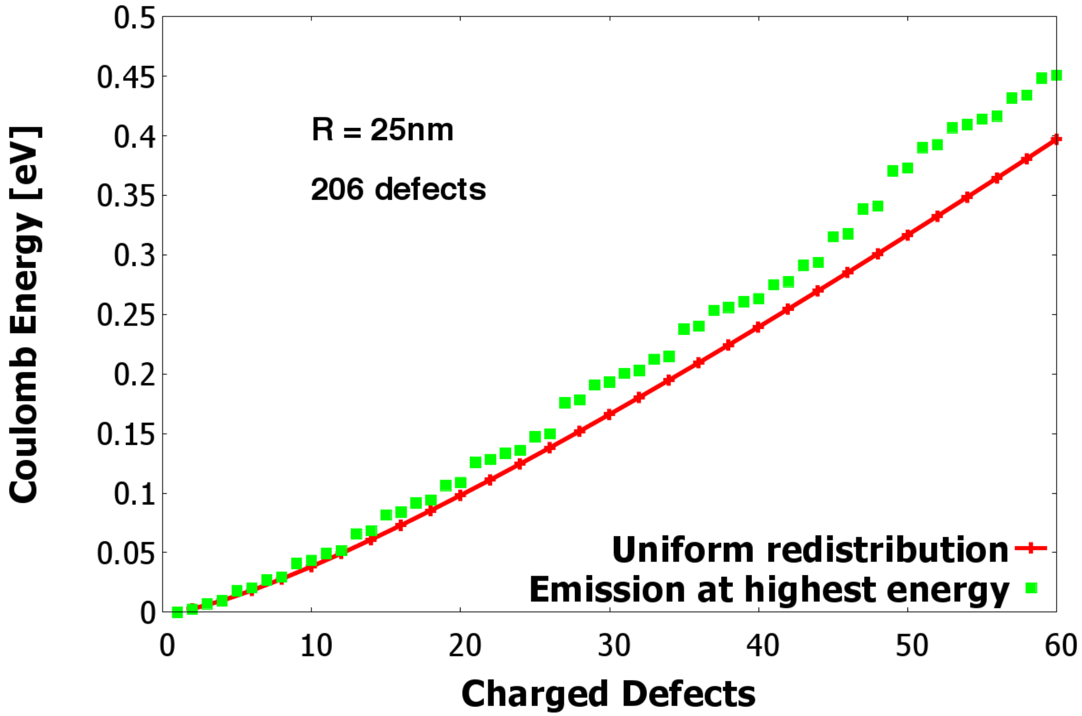

- Isotropic distribution only possible for fast equilibration in the deep level system ($\Gamma_i \ll e_n^{-1}$).
- Here the opposite case: $\Gamma_i \gg e_n^{-1}$
- Coulomb energy as function of number of charged defects very similar in both cases.
- Only lower part of the spectrum is occupied after the filling pulse.
- Green curve: starting with fully charged loop, a randomly selected site is emptied. The Coulomb energy is updated and the site with highest energy is emptied, a.s.o.

Model refinement (3)

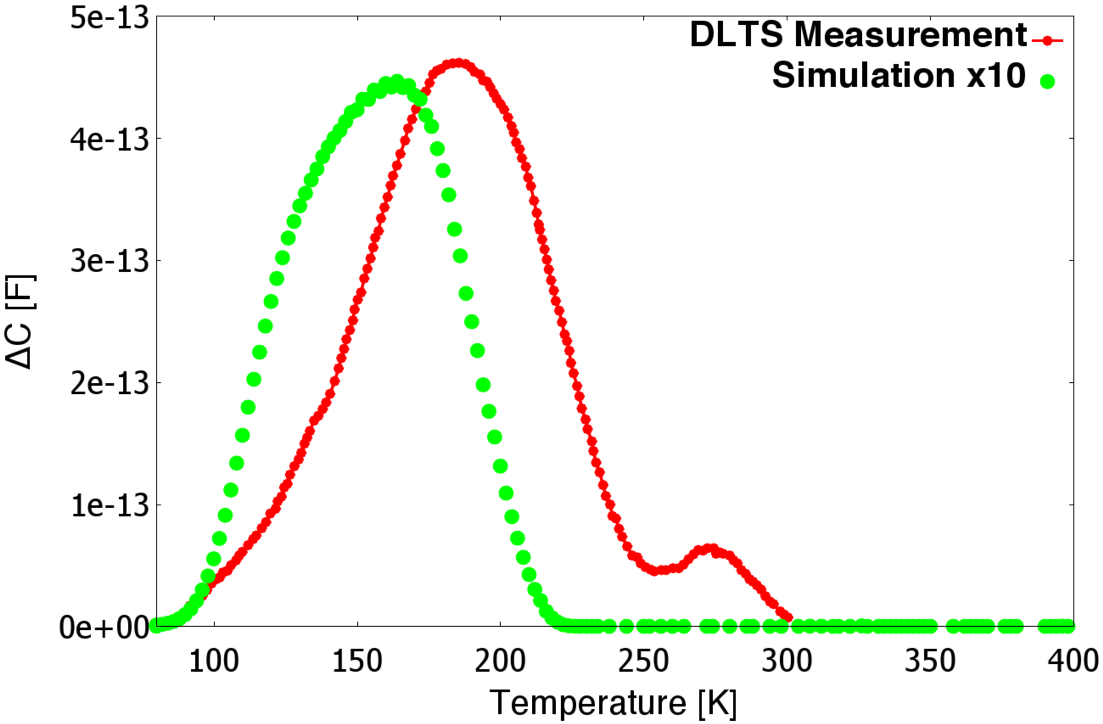

- DLTS simulation of the Schottky diode with all quantities extracted from Sentaurus-Device.
- Cascade process from Coulomb levels assumed.
- $E_T = E_C - 0.35$ eV, σ_n = 1e-15 cm^2, R & profile from process simulation
- Broadening and energetic shift.
- New E_T would be $\approx E_C - 0.4$ eV

Conclusion

Conclusion

- Based on the information of one broadened DLTS peak we suggest:
  - The generation behavior of DLs is due to decoration with point-like defects along the perimeter (transition metals, oxygen,…).
  - The states of trapped electrons are localized.
  - The proximity of the trapped point charges causes a (non-equidistant) Coulomb ladder of energy levels (Coulomb repulsion, Hartree energy).
  - During release pulse electrons are emitted in a cascade process so that the highest occupied energy level moves downwards.
  - This results in the observed broadening, but also in a deeper ground state energy E_T.

Source junction leakage (DIBL)

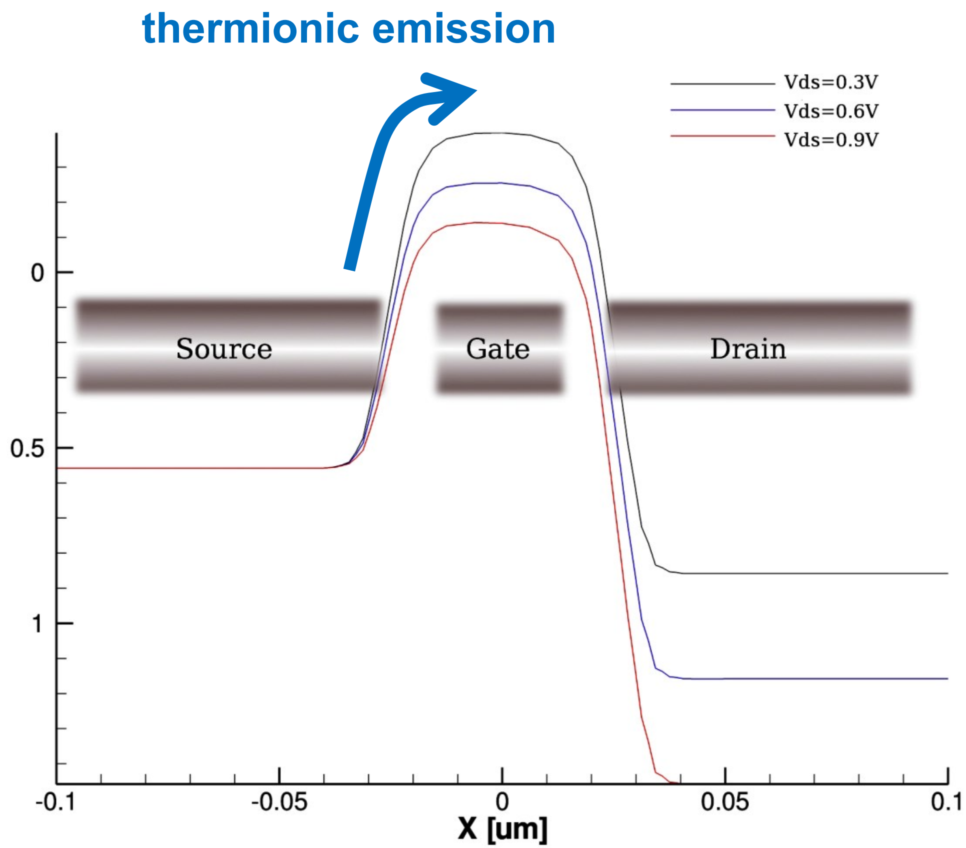

BSIM model

$$I_{subt} = I_0\, e^{\frac{V_{gs}-V_{th}}{mV_T}} \left[1 - e^{-\frac{V_{ds}}{V_T}}\right]$$

$$m = 1 + \frac{C_{dm}}{C_{ox}}$$

$$I_0 = \mu_{eff} C_{ox} \frac{W}{L} (m-1)(V_T)^2$$

DIBL empirically by

$$\Delta V_{\text{th}} \propto \gamma V_{\text{ds}}$$

Y. Taur and T. Ning. Fundamentals of Modern VLSI Devices. Cambridge University Press, dec 1998.

Band-to-band tunneling (GIDL)

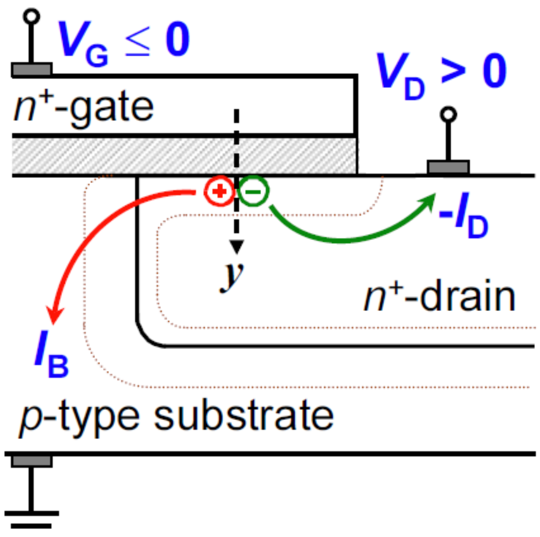

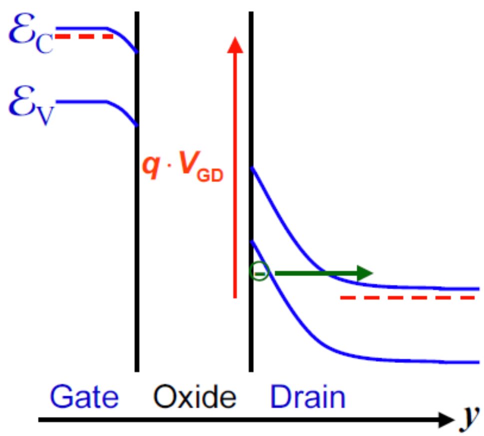

- "*Dynamic Nonlocal Path BTBT Model*" of **Sentaurus-Device** from Synopsys.

$$R_{\text{net}}^{\text{BTBT}} = A\,F^2 \exp\left(-\int_0^l \kappa\,dx\right)\left[f\left(E_{\text{F,n}}(l)\right) - f\left(E_{\text{F,p}}(0)\right)\right]$$

$$\longrightarrow A\,F^2 \exp\left(-\frac{B}{F}\right)\left[f\left(E_{\text{F,n}}(l)\right) - f\left(E_{\text{F,p}}(0)\right)\right] \quad \text{for constant F}$$

- WKB expression with numerical action integral and tunneling path dynamically searched for. Carrier generation at the classical turning points => *spatial separation between electrons and holes*.

- "*Schenk Model*"

$$R_{\text{net}}^{\text{bb}} = AF^{7/2}\frac{\tilde{n}\tilde{p} - n_{\text{i, eff}}^2}{(\tilde{n} + n_{\text{i,eff}})(\tilde{p} + n_{\text{i,eff}})}\left[\frac{(F_C^{\mp})^{-3/2}\exp\left(-\frac{F_C^{\mp}}{F}\right)}{\exp\left(\frac{\hbar\omega}{kT}\right) - 1} + \frac{(F_C^{\pm})^{-3/2}\exp\left(-\frac{F_C^{\pm}}{F}\right)}{1 - \exp\left(-\frac{\hbar\omega}{kT}\right)}\right]$$

- Various fit expressions without occupation factors

E. O. Kane, J. Phys. Chem. Solids 12, 181 (1959)

A. Schenk, "Rigorous Theory and Simplified Model of the Band-to-Band Tunneling in Silicon", Solid-State Electronics, vol. 36 (1), pp. 19-34 (1993).

Synopsys Inc., Sentaurus-Device User Guide, version 2013.03, Mountain View, California, (2013).

Gate-oxide tunneling

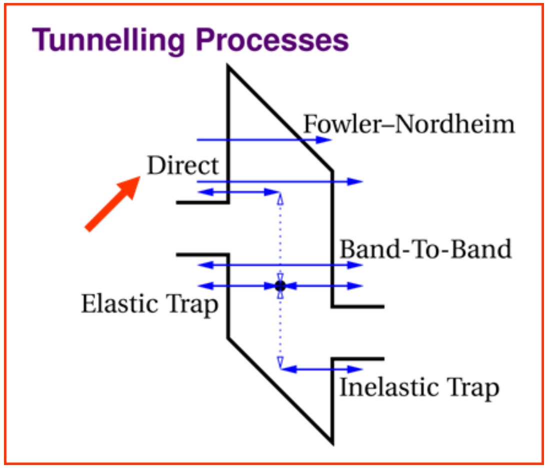

- Example: capture rate for multi-phonon-assisted tunneling via oxide traps

$$c^{n}_{\mathrm{C,phonon}} = \frac{\sqrt{m_t m_0^3 k^3 T_n^3 g_{\mathrm{C}}}}{\hbar^3 \sqrt{\chi}} V_{\mathrm{T}} S^2 \omega \left(1 - \frac{l}{S}\right)^2 \exp\left[-S(f_{\mathrm{B}}+1) + \frac{\Delta E}{2kT} + \chi\right] \times \left(\frac{z}{l+\chi}\right)^l F_{1/2}\left(\frac{E_{\mathrm{F},n} - E_{\mathrm{C}}(0)}{kT_n}\right) \frac{|\Psi(z_o)|^2}{|\Psi(0)|^2}$$

in-tunneling (OFF-state)

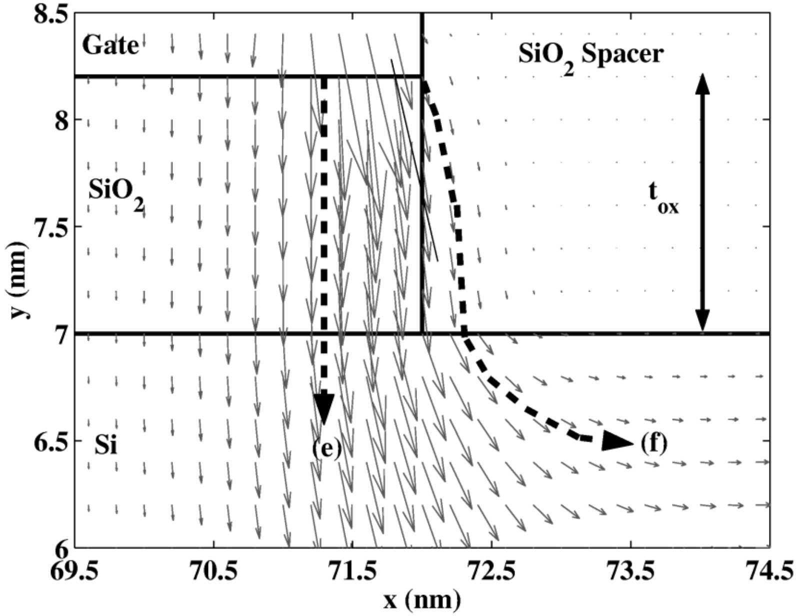

- Corner effect (drain-side gate edge).
- Only full quantum-mechanical treatment can cover the 2D nature.

Synopsys Inc., Sentaurus-Device User Guide, version 2013.03, Mountain View, California, (2013).

A. Schenk and M. Luisier, "2D Simulation of Gate Currents in MOSFETs: Comparison between S-Device and the Quantum Mechanical Simulator GreenSolver", SISPAD 2008, pp. 7-7-1 - 7-7-4.

USJ leakage simulation of industrial samples

Structured samples from ST

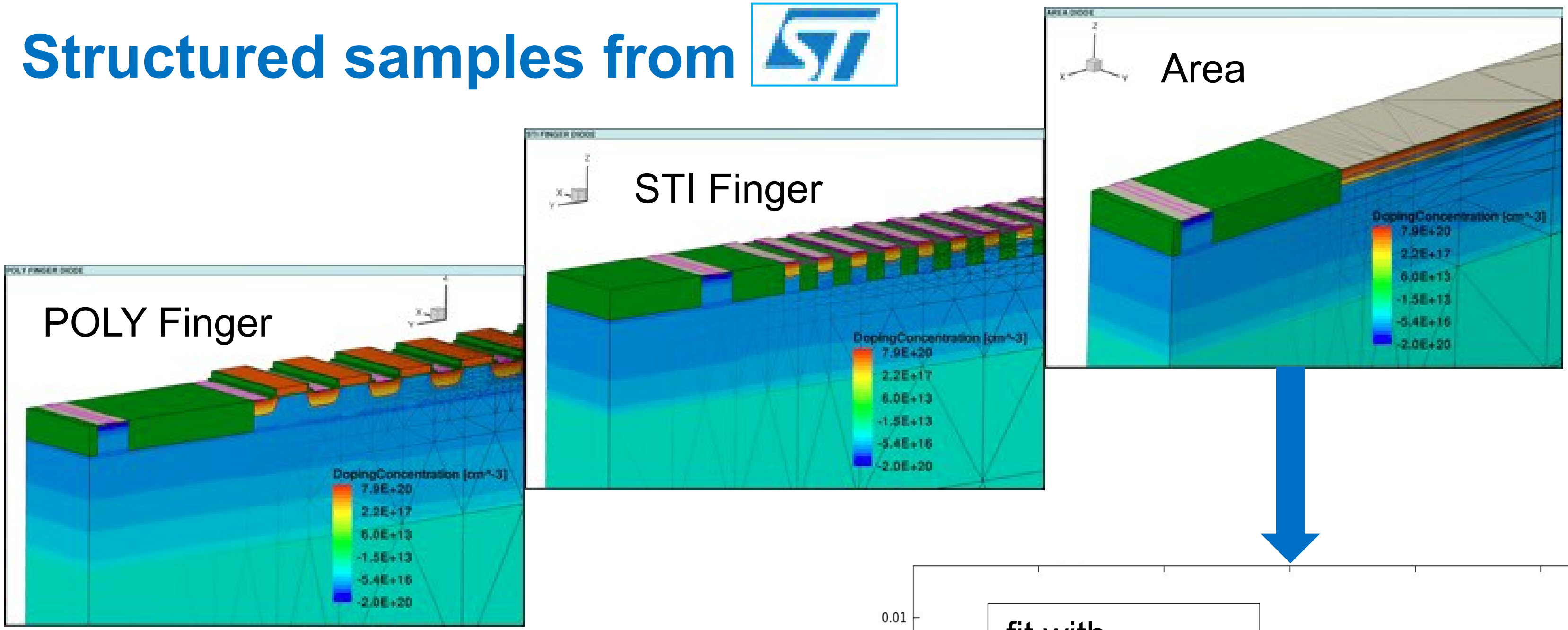

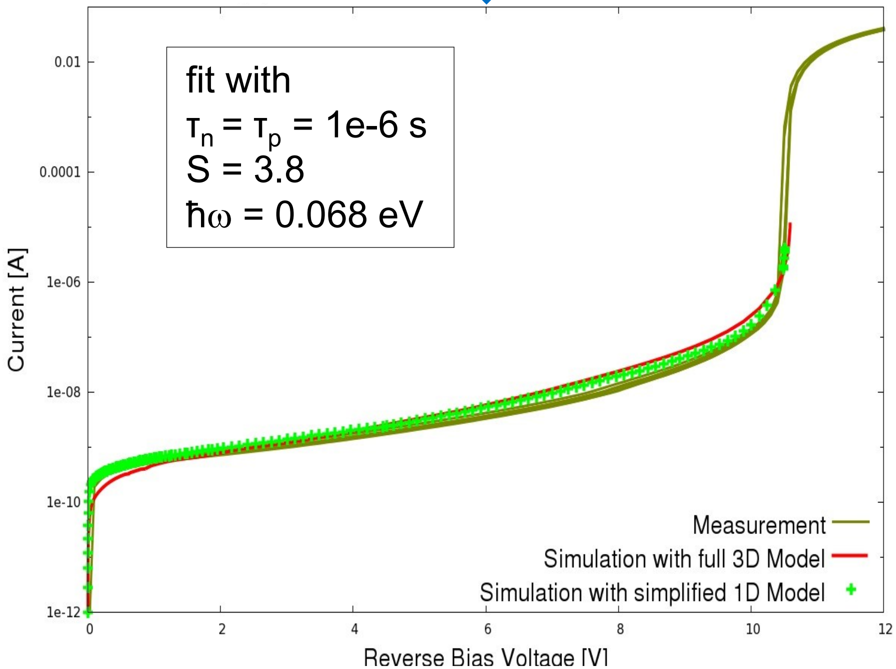

- Structured industrial samples show unspectacular TAT pre-breakdown.
- Common lifetimes and TAT parameters (similar to Si:Au default).
- Strong deviations only for certain poly finger samples which are easily explained by BTBT.

Correlation with Dislocation Loops?

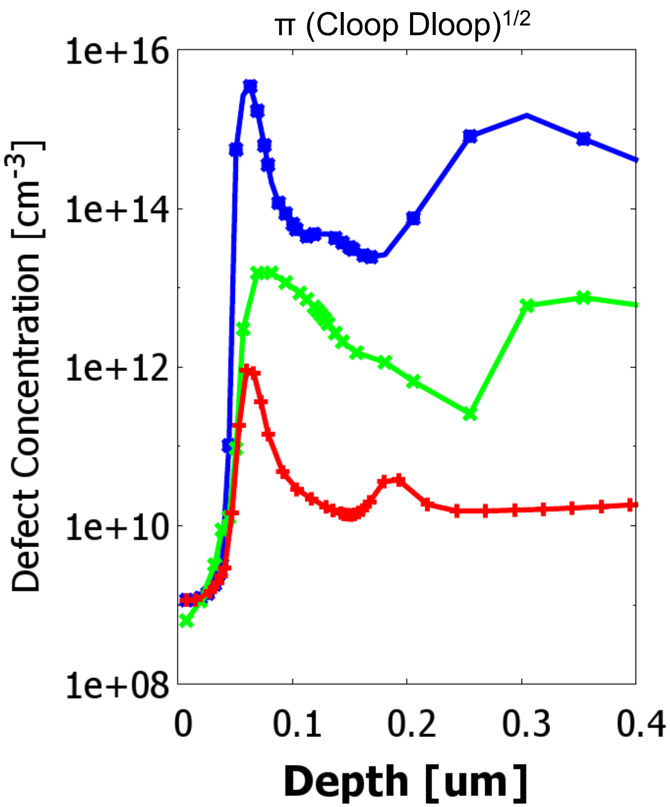

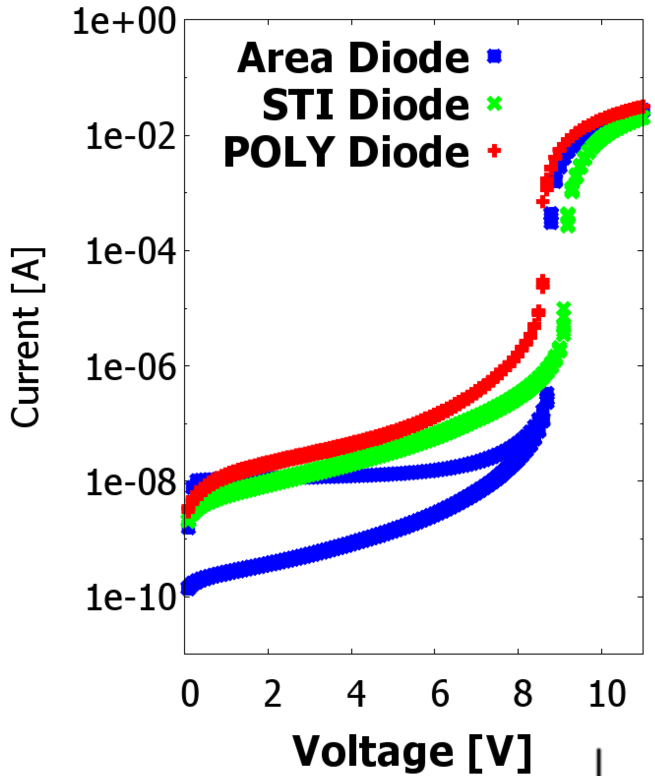

S-Process simulations and leakage measurements by Pierre Boulenc and Zahi Essa, ST Crolles, ATEMOX

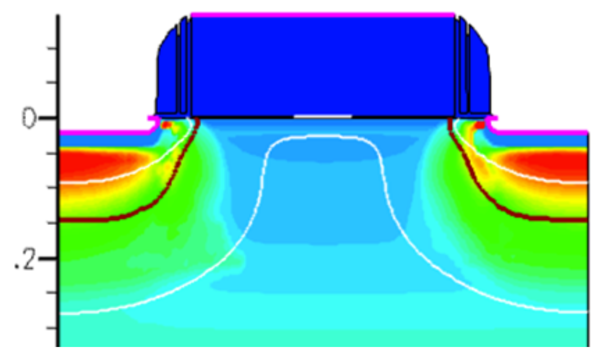

- There is a clear anti-correlation.
- **Hypothesis: DLs act as gettering centers and clean SCR from point-like defects.**